International Journal of Environmental Sciences
ISSN: 2229-7359
Vol. 12 No. 1, 2026
https://theaspd.com/index.php

Optimization of Oxidant Type, Acid Dopant, and Molar Ratio for Controlling the Structural and Electrical Properties of Polyaniline

Salim Bouhank[1*], Noreddine Medjdoub[2], Mounira Boufenghour[1], Sorya Nekkaa[2], Ismahane Tebib[1]
[1] Laboratory of Advanced Materials Technology Department of Materials Engineering National Polytechnic School of Constantine
[2] Laboratoire de Physico-Chimie des Hauts Polymères, Département de Génie des Polymères, Institut des Sciences et Techniques des Matériaux, Université Sétif, bouhanksalim@hotmail.fr

Abstract : *polyaniline is one of the most attractive intrinsically conducting polymers due to its easy synthesis, environmental stability, and tunable electrical properties. In this work, PANI was chemically synthesized by oxidative polymerization in acidic medium by varying the oxidant type (Ferric chloride or Potassium permanganate), acid dopant (Hydrochloric acid or Sulfuric acid), and aniline/oxidant molar ratio (1:1 and 1:2). The obtained samples were characterized by FTIR, XRD, UV–Vis, TGA, and four-point probe conductivity measurements. FTIR confirmed the successful formation of PANI, while XRD revealed a semi-crystalline structure with crystallite sizes ranging from 4.733 to 6.514 nm. Electrical conductivity strongly depended on synthesis conditions, reaching a maximum value of 4.739 S·cm⁻¹. UV–Vis analysis confirmed the formation of polaronic charge carriers, and TGA demonstrated good thermal stability with degradation temperatures above 500 °C. These results highlight the key role of synthesis parameters in controlling the structural organization and electrical performance of PANI.*

Keywords: *Polyaniline; Oxidative polymerization; Acid doping; Crystallinity; Electrical conductivity; Thermal stability*

INTRODUCTION

Over the past several decades, conducting polymers (CPs) have gained increasing attention owing to their strong potential as alternatives to their inorganic counterparts, leading to significant fundamental and practical research efforts[1]. A conjugated carbon chain consists of alternating single and double bonds, where the highly delocalized, polarized, and electron-dense p bonds are responsible for its electrical and optical behavior [2]. CPs provide the advantages of chemical diversity, light weight, low cost, flexibility, corrosion resistance, easy-to-control shape and morphology, and tunable conductivity over their existing inorganic counterparts [1,3]. These materials have attracted extensive research due to their potential in applications such as health-monitoring and implantable medical devices, robotic smart skin, wearable energy storage devices, human-machines interfaces, and wearable and flexible electronic systems [4].

Typical conducting polymers include polyacetylene (PA), polyaniline (PANI), polypyrrole (PPy), polythiophene (PTH), poly(para-phenylene) (PPP), poly(- phenylenevinylene) (PPV), and polyfuran (PF)... [2]. Among the available ICPs, polyaniline (PANI) has attracted considerable attention owing to its easier synthesis, low cost monomer, tunable properties, and better stability compared to other ICPs. Consequently, considerable research efforts have been devoted to the synthesis, characterization, and applications of polyaniline and its composites [6,7,8,9,10]. However, the main problem associated with the effective utilization of all ICPs including PANI is inherent in their lower level of conductivity compared to metal, and their infusibility and poor solubility in all available solvents [6]. Various methods have attempted to improve its processability, and two substantial attempts to overcome these disadvantages can be chemical modifications, namely, doped PANI and alternative PANI derivatives. The chemically modified PANI not only demonstrates improved processing capability, but enhanced conductivity and anti-corrosion properties compared with pure PANI[5].

PANI can be synthesized by chemical or electrochemical polymerization of monomer aniline in an acidic medium [8,11]. Nevertheless, achieving a controlled chemical synthesis remains challenging. It is governed by multiple parameters, including the nature of the oxidant, the type of dopant acid, the relative concentrations of the reactants, and the operational conditions of the polymerization. A thorough mastery of these factors enables the modulation of the polymer morphology toward highly ordered structures, thereby improving electrical conductivity and overall functional properties [12].

Within this framework, the primary objective of this work is the chemical synthesis of polyaniline via oxidative polymerization in an acidic medium. Key synthesis parameters were varied—specifically the type of acid utilized, as well as the nature and concentration of the oxidizing agent—in order to evaluate the structural, optical, and electrochemical properties of the resulting polyaniline. The adopted approach aims to establish correlations between the synthesis conditions and the measured performances, with the ultimate goal of identifying optimal combinations for electrochemical applications.

2. MATERIALS AND METHODS

2.1 Materials

Aniline monomer (99.5%), Ferric chloride ($FeCl_3$), Potassium permanganate ($KMnO_4$), Hydrochloric acid (HCl, 37%), and Sulfuric acid (H_2SO_4, 96%) were used as received without further purification. Ethanol, acetone, and distilled water were used during the purification process.

2.2 Synthesis of Polyaniline

Polyaniline was synthesized by chemical oxidative polymerization in acidic medium. Aqueous solutions of HCl and H_2SO_4 were first prepared at a concentration of 1 M. Oxidant solutions were then prepared by dissolving $FeCl_3$ or $KMnO_4$ in the corresponding acidic solutions at two aniline-to-oxidant molar ratios (1:1 and 1:2), generating eight different synthesis conditions.

In a typical synthesis, 9 mL of aniline were dissolved in 100 mL of the acidic medium (phase A). The oxidant solution (phase B) was added dropwise to phase A under continuous magnetic stirring at 5 °C using an ice bath. The polymerization reaction was maintained for 2 h, leading to the formation of a dark green precipitate corresponding to emeraldine salt PANI.

The resulting precipitate was recovered by centrifugation and filtration, followed by successive washing with ultrapure water, diluted acidic solution, and acetone in order to remove residual monomer and oligomeric species. The purified product was dried at 60 °C for 48 h and finally ground into a fine powder for further characterization.

2.3 Characterization

The chemical structure of the synthesized PANI samples was investigated by Fourier-transform infrared spectroscopy (FTIR) in the spectral range of 400–4000 cm^{-1} using an IRAffinity-1S spectrometer.

Structural analysis was performed by X-ray diffraction (XRD) using an X'Pert PRO diffractometer equipped with Cu Kα radiation (λ = 1.5406 Å), recorded over a 2θ range of 5–70°.

Optical properties were studied by UV–Vis spectroscopy using a double-beam spectrophotometer in the wavelength range of 200–1000 nm.

Thermal stability was evaluated by thermogravimetric analysis (TGA) under nitrogen atmosphere from 30 to 600 °C at a heating rate of 10 °C min^{-1}.

Electrical conductivity measurements were carried out using the four-point probe technique on compressed pellets (13 mm diameter, 1 mm thickness) prepared from 0.26 g of PANI powder under a uniaxial pressure of 30 kN.

3. RESULTS AND DISCUSSION

3.1 FTIR analysis

The Fourier Transform Infrared (FTIR) spectroscopy was used to confirm the successful formation of polyaniline and to investigate the effect of oxidant type, acid dopant, and monomer/oxidant ratio on its chemical structure.

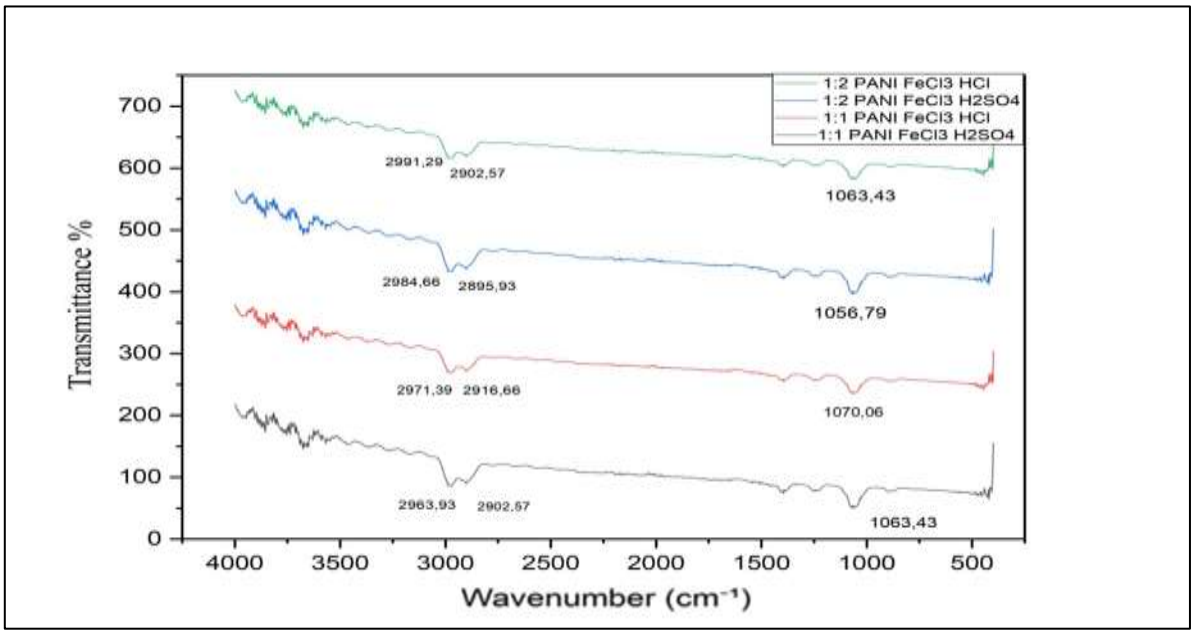

Figure 1. FTIR spectra of polyaniline samples synthesized in various acidic environments using two aniline/Ferric chloride molar ratios (1:1 and 1:2).

or samples synthesized using $FeCl_3$ as oxidant (Figure 1), characteristic absorption bands were observed in all cases, confirming the formation of the polyaniline backbone. The bands located at 2971–2916 cm^{-1} (HCl, 1:1) and 2963–2902 cm^{-1} (H_2SO_4, 1:1) correspond to aliphatic C–H stretching vibrations, generally attributed to terminal groups or residual organic species [13]. The intense band observed in the range 1070–1056 cm^{-1} is assigned to C–N stretching vibrations of secondary amine groups in doped polyaniline chains, confirming successful protonation of the polymer backbone [14].

When the molar ratio was increased to 1:2, slight shifts in band positions were observed, indicating changes in chain organization and doping level. In particular, the $FeCl_3/H_2SO_4$ (1:2) system exhibited a slightly lower intensity of the C–N band, which may indicate a lower degree of structural ordering or a predominantly amorphous organization [15].

For samples synthesized using Potassium permanganate (Figure 2), additional characteristic absorption bands were observed in the region 1597–1603 cm^{-1}, corresponding to C=N and C=C stretching vibrations of quinoid units. These bands are characteristic of the partially oxidized emeraldine structure of PANI [16]. The bands located between 1494 and 1517 cm^{-1} are attributed to C–C stretching vibrations of benzenoid units, confirming the coexistence of oxidized and reduced structural segments, typical of emeraldine salt PANI [16].

The bands observed around 1297 cm^{-1} for HCl-doped samples and 1309 cm^{-1} for H_2SO_4-doped samples are attributed to C–N stretching vibrations of secondary aromatic amines, confirming the presence of benzenoid and quinoid repeating units in the polymer chains [17]. In addition, the absorption bands located in the 634–696 cm^{-1} region correspond to in-plane and out-of-plane C–H bending vibrations of aromatic rings [18].

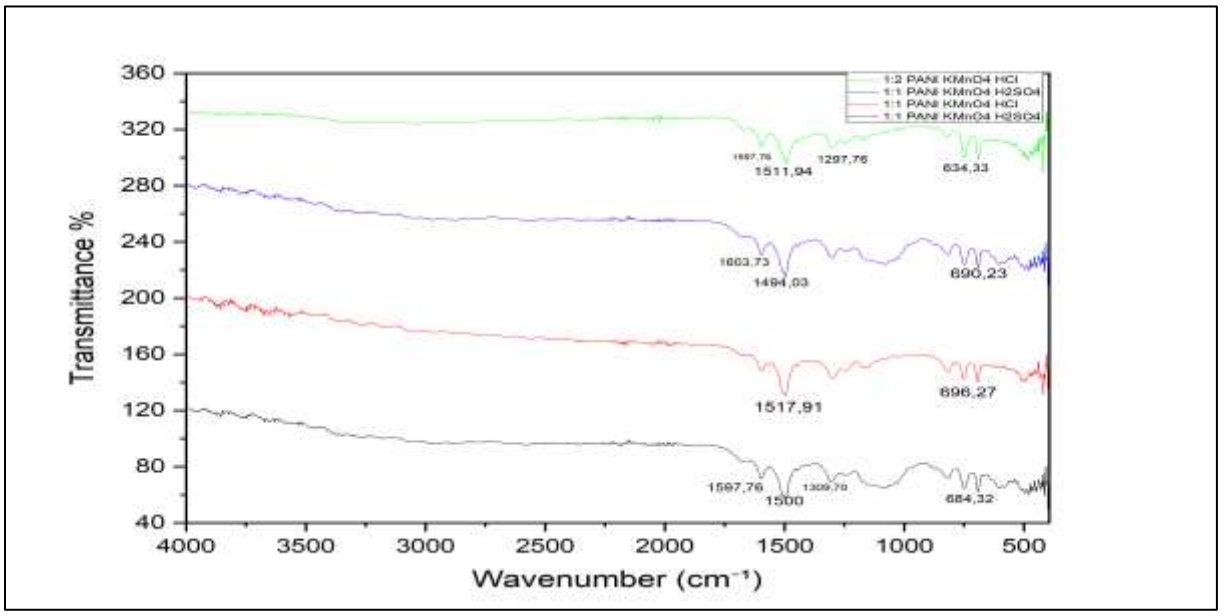

Figure 2. FTIR spectra of polyaniline samples synthesized in different acidic environments using aniline/$KMnO_4$ molar ratios of 1:1 and 1:2.

Overall, FTIR analysis confirms the successful formation of emeraldine salt PANI under all synthesis conditions and demonstrates that the oxidant type, acid dopant, and molar ratio significantly influence the doping level and structural ordering of the polymer.

3.2 X-ray diffraction analysis

Figures 3 and 4 present the X-ray diffraction patterns of polyaniline samples synthesized using Ferric chloride and Potassium permanganate as oxidizing agents, respectively, under different acidic environments (HCl and H_2SO_4) and aniline/oxidant molar ratios (1:1 and 1:2).

The obtained diffraction patterns exhibit characteristic peaks in the 2θ range of approximately 19–28°, confirming the semi-crystalline nature of PANI under all synthesis conditions. In particular, diffraction peaks located around 25°, 26°, and 27° are commonly associated with the (110), (200), and (121) crystallographic planes of emeraldine salt PANI, respectively [19]. These reflections indicate a periodic structural organization resulting from the regular stacking of benzenoid and quinoid units along the polymer backbone.

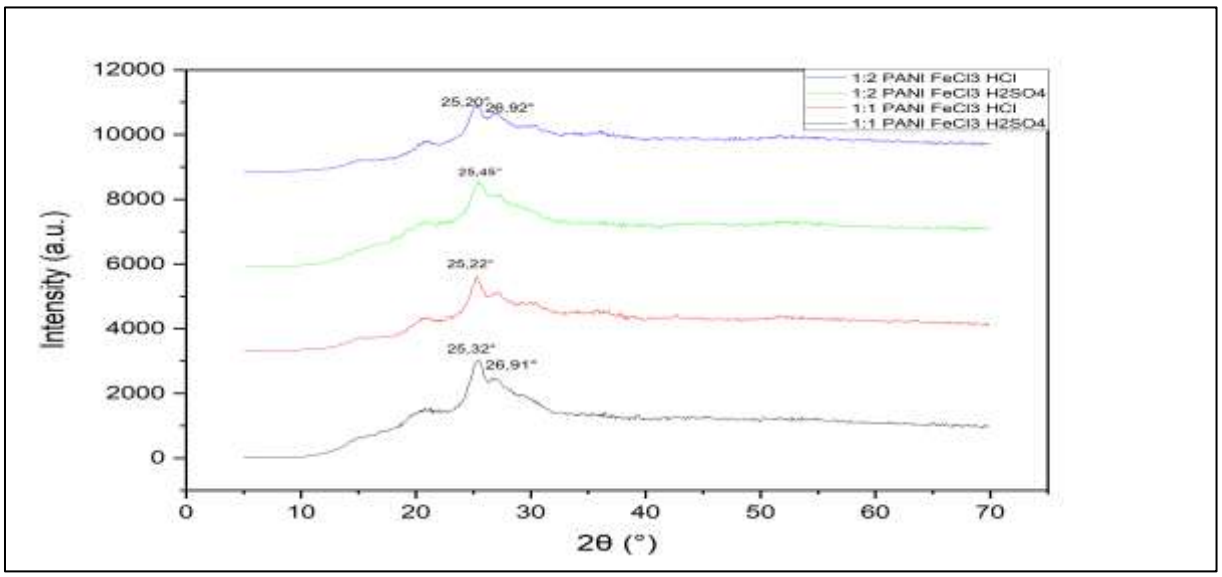

Figure 3. XRD patterns of polyaniline samples synthesized using Ferric chloride as oxidant under different acidic conditions and aniline/$FeCl_3$ molar ratios (1:1 and 1:2).

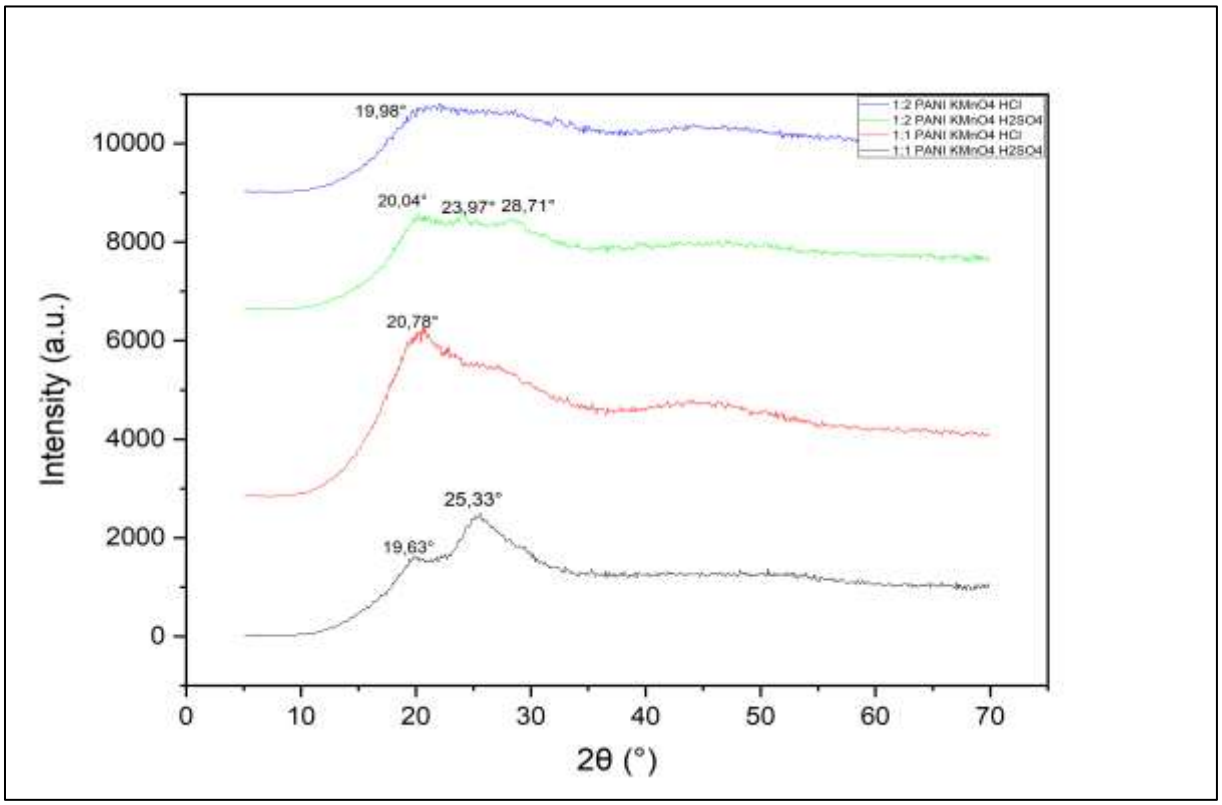

Figure 4. XRD patterns of polyaniline samples synthesized using Potassium permanganate as oxidant under different acidic conditions and aniline/$KMnO_4$ molar ratios (1:1 and 1:2).

The average crystallite size of the synthesized PANI samples was estimated using the Scherrer equation [19]:

$$L = \frac{K.\lambda}{\beta.\cos\theta}$$

where L is the crystallite size, K is the shape factor (0.94), λ is the X-ray wavelength (Cu Kα, λ = 1.5406 Å), β is the full width at half maximum (FWHM), and θ is the Bragg diffraction angle. The calculated crystallite sizes are summarized in Table 1.

Table 1. XRD parameters of synthesized PANI samples

Sample	Acid dopant	Aniline/oxidant ratio	Main diffraction peaks (2θ, °)	Crystallite size (nm)
$FeCl_3$–HCl	HCl	1:1	25.22	6.514
$FeCl_3$–HCl	HCl	1:2	25.20	5.620
			26.92	
$FeCl_3$–H_2SO_4	H_2SO_4	1:1	25.32	5.375
			26.91	
$FeCl_3$–H_2SO_4	H_2SO_4	1:2	25.45	5.583
$KMnO_4$–HCl	HCl	1:1	20.78	4.933
$KMnO_4$–HCl	HCl	1:2	19.98	4.733
$KMnO_4$–H_2SO_4	H_2SO_4	1:1	19.63	6.237
			25.33	
$KMnO_4$–H_2SO_4	H_2SO_4	1:2	20.04	6.040
			23.97	
			28.71	

a) Effect of molar ratio

By comparing samples synthesized using the same oxidant and acid dopant but different molar ratios (1:1 and 1:2), slight variations in peak position and crystallite size were observed.

For HCl-doped samples synthesized with $FeCl_3$, the main diffraction peak remained nearly constant around 25.2°, while the crystallite size slightly decreased from 6.514 nm for the 1:1 ratio to 5.620 nm for the 1:2 ratio, suggesting a slight reduction in crystalline ordering under excess oxidant conditions.
A similar behavior was observed for H_2SO_4-doped samples, where only minor variations in peak position and crystallite size were detected. In the $KMnO_4$/HCl system, a more pronounced peak shift was observed from 20.78° (1:1) to 19.98° (1:2), accompanied by a decrease in crystallite size from 4.933 to 4.733 nm.
These results indicate that the molar ratio slightly affects the interplanar spacing and crystallite growth, without significantly altering the overall semi-crystalline structure of PANI.

b) Effect of oxidant type

The oxidant type exhibited a more significant influence on the crystalline structure of PANI. Samples synthesized using $FeCl_3$ showed sharper and more intense diffraction peaks centered around $2\theta \approx 25°$, corresponding to the periodicity perpendicular to the polymer chains and indicating improved crystalline organization and better interchain packing [16].
In contrast, samples synthesized using $KMnO_4$ displayed broader diffraction peaks shifted toward lower diffraction angles (≈19–21°), characteristic of a more disordered or partially amorphous structure with smaller crystallite domains, which may result from a less controlled polymerization process [20].

c) Effect of acid dopant

The acid dopant also influenced the structural organization of PANI.
In the $FeCl_3$ system, HCl-doped samples exhibited slightly larger crystallite sizes (5.620–6.514 nm) compared with H_2SO_4-doped samples (5.375–5.583 nm), suggesting improved chain packing and a slightly more ordered structure in the presence of hydrochloric acid.
Conversely, in $KMnO_4$-based systems, H_2SO_4 promoted the formation of larger crystallites (6.040–6.237 nm) compared with HCl-doped samples (4.733–4.933 nm), suggesting enhanced interchain interactions and improved structural ordering under sulfate doping conditions.
Overall, XRD analysis confirms that the oxidant type is the dominant parameter governing the crystalline organization of PANI, while the acid dopant and molar ratio provide secondary modulation of crystallite growth and chain packing.

3.3 Electrical conductivity analysis

The electrical conductivity (σ) of the synthesized polyaniline samples was calculated from the measured electrical resistivity (ρ) according to:

$$\sigma = \frac{1}{\rho}$$

where σ is the electrical conductivity ($S \cdot cm^{-1}$) and ρ is the electrical resistivity (Ω·cm). The obtained electrical parameters are summarized in Table 2.

Table 2. Electrical parameters of synthesized PANI pellets

Sample	Aniline/oxidant r	Acid dopant	Surface resistance, Rs (Ω)	Electrical resistivity (Ω.cm)	Electrical conductivity ($S.cm^{-1}$)
PANI/$FeCl_3$	1 : 1	HCl	9,833	0,288	3,472
PANI/$KMnO_4$			9,743	0,265	0,774
PANI/$FeCl_3$		H_2SO_4	9,792	0,286	3,497
PANI/$KMnO_4$			10,092	0,295	3,390

PANI/$FeCl_3$	1 : 2	HCl	9,541	0,279	3,367
PANI/$KMnO_4$			9,639	0,211	4,739
PANI/$FeCl_3$		H_2SO_4	9,728	0,277	3,610
PANI/$KMnO_4$			9,724	0,285	3,508

a) Effect of molar ratio

The influence of the aniline/oxidant molar ratio on electrical conductivity was generally limited, except for the $KMnO_4$-based system. In HCl medium, the conductivity of PANI synthesized using $KMnO_4$ increased significantly from 0.774 $S{\cdot}cm^{-1}$ at the 1:1 ratio to 4.739 $S{\cdot}cm^{-1}$ at the 1:2 ratio, indicating that excess oxidant strongly enhances charge transport under these synthesis conditions. In contrast, $FeCl_3$-based samples exhibited relatively stable conductivity values regardless of the molar ratio, varying between 3.367 and 3.610 $S{\cdot}cm^{-1}$.

b) Effect of oxidant type

The oxidant type exhibited a major influence on the electrical properties of PANI. Under comparable synthesis conditions, $FeCl_3$ generally produced higher conductivity values than $KMnO_4$, which is consistent with the XRD results showing sharper diffraction peaks and improved crystalline ordering for $FeCl_3$-based samples. For example, at the 1:1 molar ratio in H_2SO_4 medium, $FeCl_3$ yielded a conductivity of 3.497 $S{\cdot}cm^{-1}$, compared with 3.390 $S{\cdot}cm^{-1}$ for $KMnO_4$. This behavior may be attributed to a more controlled oxidation process, promoting better chain conjugation and electron delocalization within the polymer backbone.

c) Effect of acid dopant

The acid dopant also affected the electrical conductivity of PANI. In $FeCl_3$-based systems, H_2SO_4-doped samples systematically exhibited slightly higher conductivity than HCl-doped samples, suggesting a more efficient protonation and improved charge carrier mobility.

However, an exceptional behavior was observed for the $KMnO_4$/HCl system at the 1:2 ratio, where the highest conductivity of 4.739 $S{\cdot}cm^{-1}$ was obtained, exceeding all other formulations. This result suggests a synergistic effect between permanganate oxidation, hydrochloric acid doping, and excess oxidant concentration, possibly leading to improved microstructural connectivity and enhanced polaron transport.

Overall, electrical conductivity measurements confirm that the oxidant type is the primary parameter governing charge transport in PANI, while the acid dopant and molar ratio provide secondary but non-negligible modulation of the electrical performance.

3.4 UV–Visible analysis

Figures 5 and 6 present the UV–Visible absorption spectra of selected polyaniline samples synthesized at an aniline/oxidant molar ratio of 1:1 using different oxidizing agents and acid dopants. UV–Vis spectroscopy was employed to investigate the electronic structure and doping state of the synthesized PANI through the identification of characteristic electronic transitions.

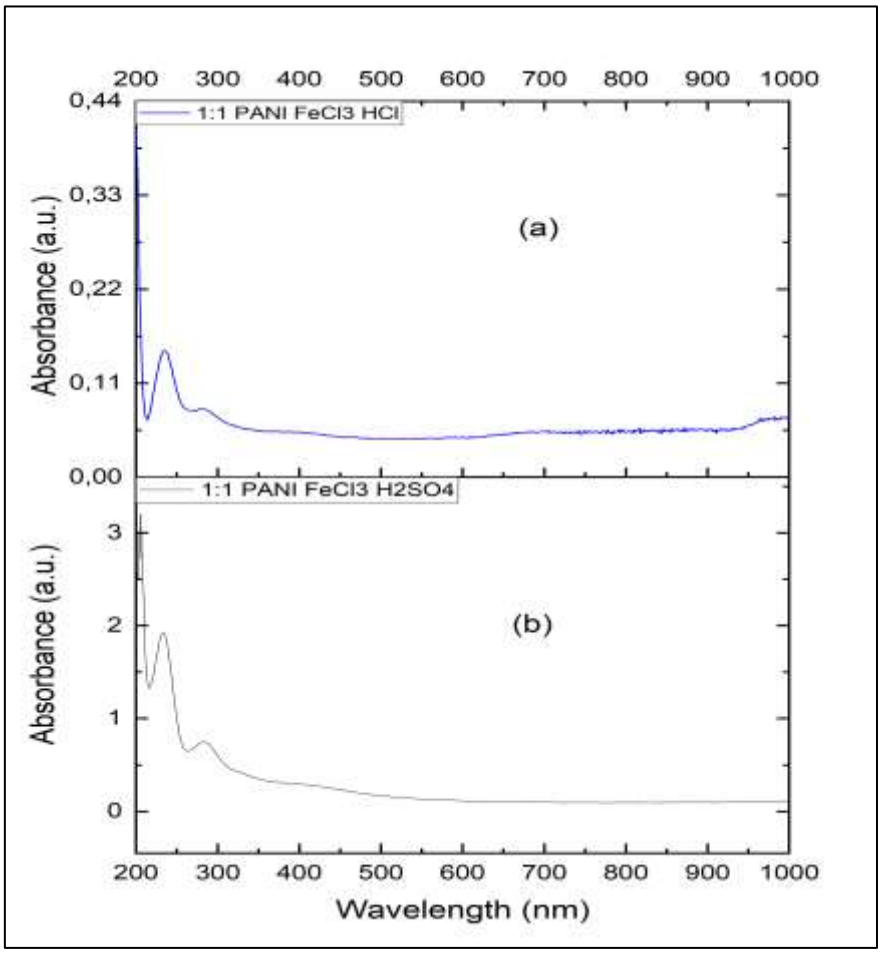

Figure 5. UV–Visible spectra of PANI samples synthesized using Ferric chloride at an aniline/$FeCl_3$ molar ratio of 1:1:

(a) HCl-doped sample;
(b) H_2SO_4-doped sample.

For the $FeCl_3$/HCl sample (Figure 5a), an absorption band centered at approximately **237 nm** was observed, corresponding to the π–π* electronic transition of benzenoid rings, characteristic of neutral or weakly oxidized segments within the PANI backbone [21,22,23]. The absence of a significant absorption band at higher wavelengths suggests a moderate doping level, which is consistent with its measured electrical conductivity of **3.472 S·cm⁻¹**.

In contrast, the $FeCl_3$/H_2SO_4 sample (Figure 5b) exhibited two distinct absorption bands located at approximately **232 nm** and **285 nm**. The first band corresponds to the π–π* transition of benzenoid units, while the second may be assigned to a polaron–π* transition, indicating a higher oxidation and protonation level compared with the HCl-doped sample [21,23]. This observation is in agreement with its slightly higher conductivity (**3.497 S·cm⁻¹**) and suggests enhanced generation of polarons, which act as mobile charge carriers within the polymer chains [22].

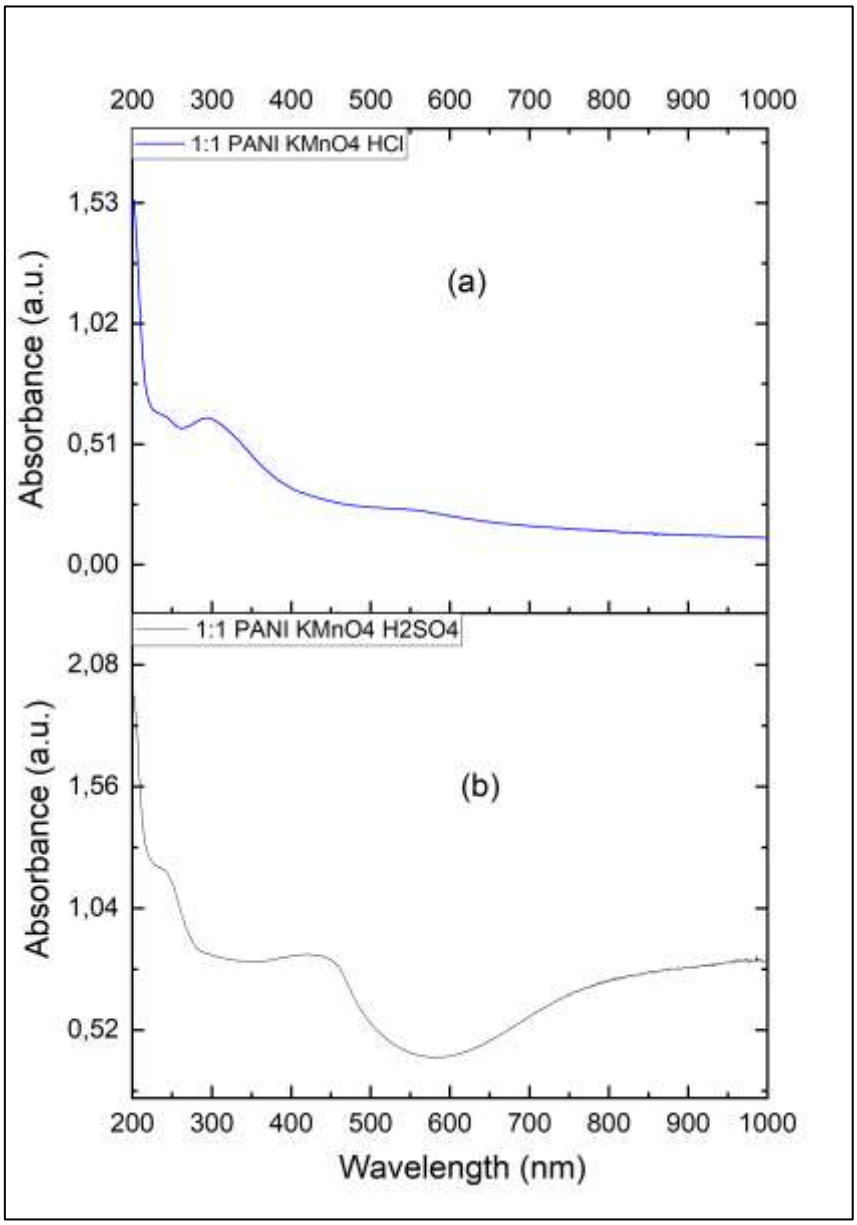

Figure 6. UV–Visible spectra of PANI samples synthesized using Potassium permanganate at an aniline/$KMnO_4$ molar ratio of 1:1:

(a) HCl-doped sample;
(b) H_2SO_4-doped sample.

For the $KMnO_4$/HCl sample (Figure 6a), a single absorption band was observed at approximately **290 nm**, which may be attributed to overlapping π–π* and polaron–π* transitions. The shift toward higher wavelength compared with the $FeCl_3$/HCl system suggests partial oxidation and moderate protonation of the polymer backbone. However, the absence of a broad polaronic absorption band indicates incomplete charge delocalization, which is consistent with the relatively low conductivity measured for this sample (**0.774 S·cm⁻¹**) [24].

In the case of the $KMnO_4$/H_2SO_4 sample (Figure 6b), an intense absorption band appeared at approximately **440 nm**, accompanied by a broad absorption shoulder around **243 nm**. The band at 440 nm is characteristic of polaron–π* transitions and confirms the presence of a highly protonated emeraldine salt structure with a significant concentration of mobile charge carriers [22,24]. This result is fully consistent with the relatively high electrical conductivity obtained for this sample (**3.390 S·cm⁻¹**) and indicates that the combined effect of $KMnO_4$ oxidation and H_2SO_4 doping promotes efficient electronic delocalization within the polymer matrix [21,23].

Overall, UV–Visible analysis confirms that the oxidant type and acid dopant strongly influence the electronic structure and doping level of PANI. Samples exhibiting pronounced polaronic absorption bands systematically showed higher electrical conductivity, confirming the strong correlation between protonation level, charge carrier formation, and electrical performance.

3.5 Thermogravimetric analysis

Figures 7 and 8 present the thermogravimetric (TGA) and derivative thermogravimetric (DTG) curves of selected polyaniline samples synthesized at an aniline/oxidant molar ratio of 1:1 using different oxidizing agents and acid dopants. Thermal analysis was performed to evaluate the thermal stability of the synthesized PANI and to investigate the influence of synthesis parameters on its degradation behavior.

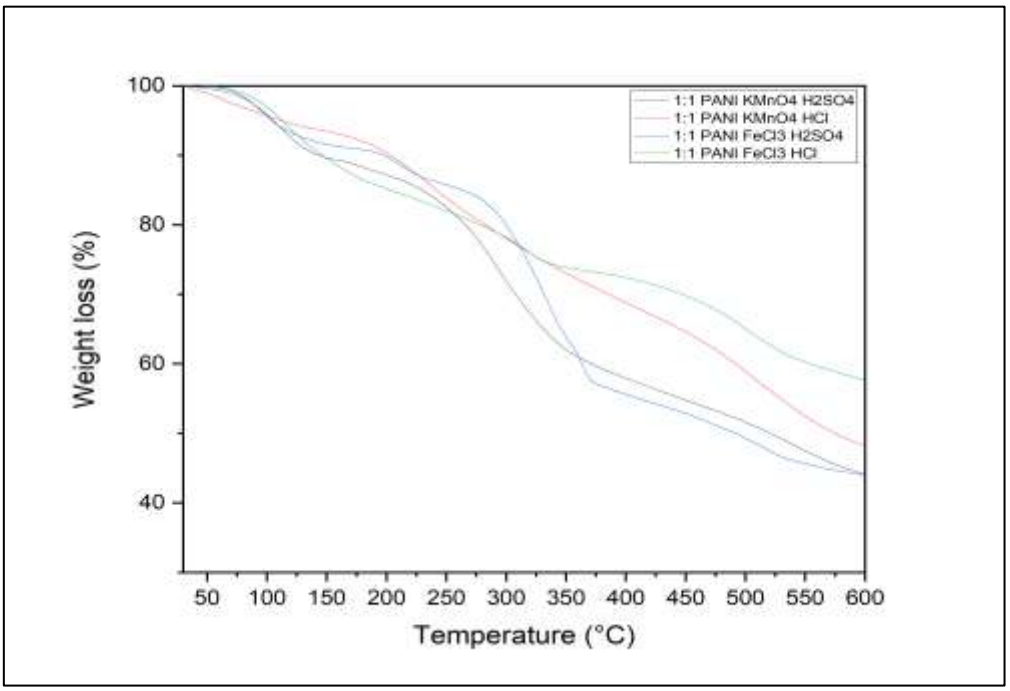

Figure 7. TGA thermograms of PANI samples synthesized at an aniline/oxidant molar ratio of 1:1 using different oxidizing agents and acidic media (HCl and H_2SO_4).

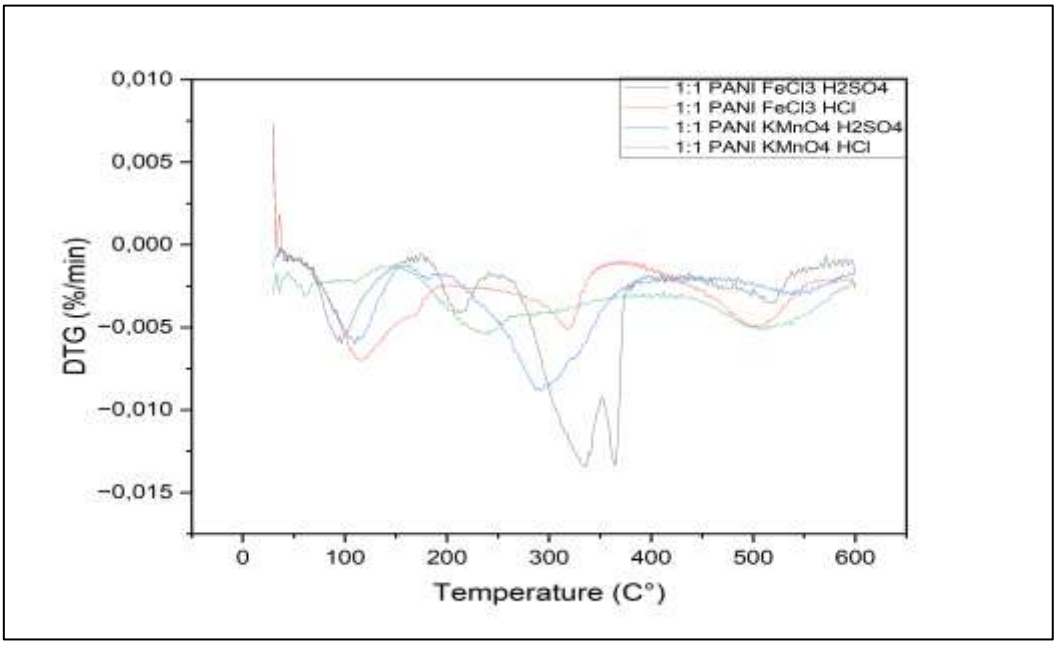

Figure 8. DTG thermograms of PANI samples synthesized at an aniline/oxidant molar ratio of 1:1 using different oxidizing agents and acidic media (HCl and H_2SO_4).

All investigated samples exhibited a typical three-step thermal degradation behavior, as clearly observed from the DTG profiles. This degradation pattern is consistent with previous reports on chemically synthesized acid-doped PANI [25,26].

The first weight-loss stage occurred in the temperature range of approximately **70–130 °C** and is attributed to the removal of physically adsorbed moisture, residual solvent molecules, free acid dopants, and traces of unreacted oxidizing species. This initial mass loss remained relatively low, generally below **10 wt.**%, indicating good structural stability at low temperatures.

The second degradation stage was observed between approximately **200 and 320 °C** and is generally associated with the elimination of low-molecular-weight oligomeric fragments as well as the progressive release of chemically bonded dopant species, corresponding to a gradual dedoping process. The DTG peaks observed in this region confirm a well-defined but relatively slow degradation kinetics [26].

The third and major degradation stage occurred above **350 °C** and corresponds to the thermal decomposition of the main conjugated backbone of PANI, involving the rupture of aromatic and quinoid structural units. The maximum degradation temperatures (T_{d,max}) varied significantly depending on the synthesis conditions, ranging from approximately **355 to 525 °C**, indicating that the thermal stability of PANI strongly depends on both the oxidizing agent and the acid dopant.

Among all investigated formulations, the HCl-doped samples exhibited the highest thermal stability, with a maximum degradation temperature reaching approximately **525 °C**. This enhanced thermal resistance may be attributed to stronger interchain interactions and improved structural organization, which is consistent with the XRD results showing relatively larger crystallite domains for HCl-doped $FeCl_3$-based samples.

Overall, thermogravimetric analysis confirms that the synthesized PANI samples possess good thermal stability, and demonstrates that the acid dopant plays a significant role in governing the thermal resistance of the polymer. The combination of high electrical conductivity and elevated thermal stability makes these formulations promising candidates for electrochemical and electronic applications.

4. CONCLUSION

In this study, polyaniline was successfully synthesized by chemical oxidative polymerization in acidic medium by systematically varying the oxidizing agent, acid dopant, and aniline/oxidant molar ratio. FTIR analysis confirmed the successful formation of emeraldine salt PANI under all synthesis conditions, while XRD results revealed a semi-crystalline structure with crystallite sizes ranging from **4.733 to 6.514 nm**, demonstrating that the structural organization strongly depends on the synthesis parameters.

Among the investigated variables, the oxidant type was identified as the dominant parameter governing both crystalline ordering and electrical performance. Samples synthesized using Ferric chloride generally exhibited sharper diffraction peaks and stable conductivity values between **3.367 and 3.610 S·cm⁻¹**, indicating improved chain packing and efficient charge delocalization. In contrast, Potassium permanganate produced more disordered structures, although an exceptional conductivity of **4.739 S·cm⁻¹** was achieved in the $KMnO_4$/HCl system at an aniline/oxidant ratio of 1:2, highlighting a favorable synergistic effect between oxidant concentration and protonic doping.

UV–Visible spectroscopy confirmed the formation of polaronic charge carriers in the most conductive samples, while thermogravimetric analysis demonstrated good thermal stability with degradation temperatures exceeding **500 °C** for selected formulations. Overall, these results demonstrate that the combined optimization of oxidant type, acid dopant, and molar ratio provides an effective strategy for tailoring the structural organization, charge transport behavior, and thermal stability of PANI. The optimized formulations obtained in this work show strong potential for future applications in electrochemical devices, sensors, and energy-related materials.

REFERENCES

[1] T.-H. Le, Y. Kim, H. Yoon, Electrical and Electrochemical Properties of Conducting Polymers, Polymers **9** (2017) 150.
[2] K. Namsheer, C.S. Rout, Conducting polymers: a comprehensive review on recent advances in synthesis, properties and applications, RSC Adv. **11** (2021) 5659–5697.
[3] M.H. Naveen, N.G. Gurudatt, Y.-B. Shim, Applications of conducting polymer composites to electrochemical sensors: A review, Appl. Mater. Today **9** (2017) 419–433.
[4] I.-A. Pavel, S. Lakard, B. Lakard, Flexible Sensors Based on Conductive Polymers, Chemosensors **10** (2022) 97.

[5] M. Beygisangchin, S.A. Rashid, S. Shafie, A.R. Sadrolhosseini, H.N. Lim, Preparations, Properties, and Applications of Polyaniline and Polyaniline Thin Films—A Review, Polymers **13** (2021) 2003.
[6] S. Bhadra, D. Khastgir, N.K. Singha, J.H. Lee, Progress in preparation, processing and applications of polyaniline, Prog. Polym. Sci. **34** (2009) 783–810.
[7] F.A. Rifa'i, D.K. Saputra, M. Apriliana, L.A.N. Abidin, Harjono, Synthesis, Characterization, and Applications of Polyaniline as a Conductive Polymer in Modern Technologies: A Review, Indones. J. Pure Appl. Chem. **8** (2025) 66–90.
[8] Z. Li, L. Gong, Research Progress on Applications of Polyaniline (PANI) for Electrochemical Energy Storage and Conversion, Materials **13** (2020) 548.
[9] N.A. Shawky, S.M. Abdallah, M.H. Sorour, A.M. Awad Abouelata, M.A. Abdel-Fatah, Electrochemical Polymerization of Polyaniline: A Comprehensive Review of Synthesis Conditions, Nanocomposites, and Industrial Applications, Cureus J. Eng. (2025). https://doi.org/10.7759/s44388-025-04726-2.
[10] S. Jahani, K. Boguslawski, P. Tecmer, The relationship between structure and excited-state properties in polyanilines from geminal-based methods, RSC Adv. **13** (2023) 27898.
[11] E.N. Zare, P. Makvandi, B. Ashtari, F. Rossi, A. Motahari, G. Perale, Progress in Conductive Polyaniline-Based Nanocomposites for Biomedical Applications: A Review, J. Med. Chem. **63** (2020) 1–22.
[12] J. Huang, R.B. Kaner, A General Chemical Route to Polyaniline Nanofibers, J. Am. Chem. Soc. **126** (2004) 851–855.
[13] A.G. MacDiarmid, J.C. Chiang, A.F. Richter, Polyaniline: A novel conducting polymer, Synth. Met. **18** (1987) 285–290.
[14] R.G. Gilbert, Polyaniline. Preparation of a conducting polymer (IUPAC Technical Report), Pure Appl. Chem. **74** (2002) 857–867.
[15] Y.F. Huang, C.W. Lin, Introduction of methanol in the formation of polyaniline nanotubes in an acid-free aqueous solution through a self-curling process, Polymer **50** (2009) 775–782.
[16] T. Abdiryim, X.-G. Zhang, R. Jamal, Comparative studies of solid-state synthesized polyaniline doped with inorganic acids, Mater. Chem. Phys. **90** (2005) 367–372.
[17] H.G. Taleghani, Preparation and Characterization of Polyaniline Nanoparticles Using Various Solutions, World Appl. Sci. J. **6** (2009) 1607–1611.
[18] K. Mamma, K. Siraj, N. Mek, Effect on Poly(C6H5NH2) emeraldine salt by $FeCl_3$ and $KMnO_4$ as secondary dopants, Am. J. Polym. Sci. Eng. **1** (2013) 1–13.
[19] S.A. Hasoon, S.A. Abdul-Had, Optical, Structural and Electrical Properties of Electrochemical Synthesis of Thin Film of Polyaniline, Baghdad Sci. J. **15** (2018).
[20] S. Bhadra, D. Khastgir, N.K. Singha, J.H. Lee, Progress in preparation, processing and applications of polyaniline, Prog. Polym. Sci. **34** (2009) 783–810.
[21] H. Kebiche, Etude de la synthèse par voie chimique de nanostructures de polyaniline et de nanocomposites de polyaniline/particules métalliques – Application à la détection d'ammoniac, Doctoral Thesis, 2014.
[22] M.M. Ska, C.Y. Yue, Synthesis of polyaniline nanotubes using the self-assembly behavior of vitamin C: a mechanistic study and application in electrochemical supercapacitors, J. Mater. Chem. A **2** (2014) 2830.
[23] G. Yang, F. Liu, N. Hou, S. Peng, C. He, P. Fang, Preparation of One-Dimensional Polyaniline Nanotubes as Anticorrosion Coatings, Materials **15** (2022) 3192.
[24] H. Ding, J. Shen, M. Wan, Z. Chen, Formation Mechanism of Polyaniline Nanotubes by a Simplified Template-Free Method, Macromol. Chem. Phys. **209** (2008) 864–871.
[25] A. Kumar, A. Kumar, H. Mudila, K. Awasthi, V. Kumar, Synthesis and thermal analysis of polyaniline (PANI), J. Phys. Conf. Ser. **1531** (2020) 012108.
[26] F. Yelmaz, Polyaniline: Synthesis, Characterization, Solution Properties and Composites, Ph.D. Thesis, 2007.